Molecular Crystals and Liquid Crystals
Publication details, including instructions for authors and subscription information:
http://www.tandfonline.com/loi/gmcl20

Concentration Variation of Quadratic NLO Susceptibility in PMMA-DR1 Side Chain Polymer

F. Kajzar [a] [b], O. Krupka [c], G. Pawlik [d], A. Mitus [d] & I. Rau [b]

[a] Angers University, POMA Laboratory, Angers, France

[b] Faculty of Applied Chemistry and Materials Science, University Politehnica Bucharest, Bucharest, Romania

[c] Department of Chemistry, Taras Schevchenko Kiev National University, Kiev, Ukraine

[d] Institute of Physics, Wroclaw Technical University, Nabrzeze Wyspianskiego, Wroclaw, Poland

Version of record first published: 28 May 2010

To cite this article: F. Kajzar, O. Krupka, G. Pawlik, A. Mitus & I. Rau (2010): Concentration Variation of Quadratic NLO Susceptibility in PMMA-DR1 Side Chain Polymer, Molecular Crystals and Liquid Crystals, 522:1, 180/[480]-190/[490]

To link to this article: http://dx.doi.org/10.1080/15421401003720017

Mol. Cryst. Liq. Cryst., Vol. 522: pp. 180/[480]–190/[490], 2010
Copyright © Taylor & Francis Group, LLC
ISSN: 1542-1406 print/1563-5287 online
DOI: 10.1080/15421401003720017

Taylor & Francis
Taylor & Francis Group

Concentration Variation of Quadratic NLO Susceptibility in PMMA-DR1 Side Chain Polymer

F. KAJZAR,[1,2] O. KRUPKA,[3] G. PAWLIK,[4]
A. MITUS,[4] AND I. RAU[2]

[1]Angers University, POMA Laboratory, Angers, France
[2]Faculty of Applied Chemistry and Materials Science, University Politehnica Bucharest, Bucharest, Romania
[3]Department of Chemistry, Taras Schevchenko Kiev National University, Kiev, Ukraine
[4]Institute of Physics, Wroclaw Technical University, Nabrzeze Wyspianskiego, Wroclaw, Poland

Chemical synthesis and concentration dependence of two second order NLO tensor components: $\chi_{pp}^{(2)}(-2\omega;\omega,\omega)$ *and* $\chi_{sp}^{(2)}(-2\omega;\omega,\omega)$ *was studied for a side chain polymer PMMA-DR1 in thin films by optical second harmonic generation techniques. The noncentrosymmetry was created by the corona poling technique. The results show that for small chromophore concentrations the* $\chi_{pp}^{(2)}(-2\omega;\omega,\omega)$ *susceptibility follows linearly the density number of active chromophores, reaches a maximum, than decreases and stabilizes.*

Keywords Concentration dependence of SHG susceptibility; electric field poling; NLO susceptibility; nonlinear optics; poled polymers; second harmonic generation

Introduction

Electro-optic polymers [1–3] have emerged as a new class of photonic materials for different kinds of application in second order nonlinear optical devices and particularly in optically active waveguides. They marry excellent optical quality of usually optically inactive, amorphous, polymer matrix with highly nonlinear optical active chromophores, embedded in. The necessary for this kind of applications noncentrosymmetry is obtained either by DC field [4] or by all optical poling [5]. Because of the amorphous structure and solubility these materials usually can be easily processed into good optical thin films. Such property is particular importance as most of applications are targeted waveguiding configuration.

Address correspondence to F. Kajzar, Angers University, POMA Laboratory, 2 bd Lavoisier, Angers 49045, France. Tel.: +40213154193; Fax: +40213154193; E-mail: frkajzar@yahoo.com

The research in this field is driven by numerous practical applications, such as:

- Laser frequency tuning through frequency doubling by SHG, sum, difference frequency generation, optical parametric oscillation (OPO)
- Optical parametric amplification (OPA) of weak signals
- Electrooptic modulation for optical signal transmission
- Linear rectification for generation of THz electric pulses

Several thin films preparation techniques were developed and/or applied for noncentrosymmetric thin film fabrication such as:

- Langmuir-Blodgett technique [6,7]
- Solution casting of isotropic [8] and liquid crystalline polymers [9,10]
- Epitaxial or quasi-epitaxial growth [11,12]
- Self assembly [13]
- Intramolecular charge transfer systems [14]

All these techniques present some advantages and disadvantages. Concerning the electro-optic modulation (EOM) application the best results were obtained with isotropic polymers, functionalised with highly responsive NLO chromophores [15]. High modulation rate (113 GHz), low half wavelength V_π (voltage below 1 V) [16] were demonstrated. Electro-optic modulation was also demonstrated with corrugated waveguides [17]. Also second harmonic generation (SHG) [18] and optical parametric amplification (OPA) [19] in waveguiding configuration were demonstrated. Electro-optic polymers exhibit also large third order NLO properties. A low control fluence all optical commutator was demonstrated [20].

One of the important problem encountered with electro-optic polymers is the chromiophore aggregation. In order to get second-order NLO effect the constituent chromophores have to lack center of inversion. The most efficient, known actually, are the quasi 1D charge transfer chromophores. These chromophores exhibit not only a large first hyperpolarizability β_{zzz} component, important for practical applications, but also a large ground state dipolar moment μ. A large dipole moment is important for orientation as it increases the ordering energy μE, where E is the applied poling field. But at the same time it leads to a large dipole-dipole interaction leading to their aggregation. Such aggregates are centrosymmetric with no second order NLO response. Moreover they scatter light increasing in this way the unwanted propagation losses. On the other hand the second order NLO susceptibility of a poled polymer is given by:

$$\chi^{(2)}_{IJK}(-\omega_3;\omega_1,\omega_2) = NF < \beta_{ijk}(-\omega_3;\omega_1,\omega_2) >_{IJK} \tag{1}$$

where N is the active molecules number density and F is the factor taking account of local field (crystal field) acting on molecules.

$$F = (f_\omega)^2 f_{2\omega} \tag{2}$$

For a spherical symmetry molecule

$$f^\omega = \frac{\varepsilon^\omega + 2}{3} \tag{3}$$

where ε^ω is the medium dielectric constant at ω frequency.

$<>$ is the configurational average taken over all chromophore orientations.

For poled polymers and CT chromophores, taking account of the Kleinman's relations [21], there are two nonzero $\chi^{(2)}$ tensor components given by (for details see e.g., Ref. [22]) the diagonal

$$\chi^{(2)}_{ZZZ} = NF\beta_{zzz} < \cos^3 \Theta > \tag{4}$$

and the off diagonal one

$$\chi^{(2)}_{XXZ} = \frac{1}{2} NF\beta_{zzz} < \sin\Theta \cos^2 \Theta > \tag{5}$$

where Z is direction of the poling field and Θ is angle which makes the molecular axis with Z direction.

For diagonal tensor component the configurational average $<>$ in Eq. (4) spans between zero for an isotropic system and 1 for a perfectly ordered system. In the last case of a perfectly ordered polymer with all molecular axes pointing in the same direction the off diagonal component $\chi^{(2)}_{XXZ} \equiv 0$.

According to Eq. (2) $\chi^{(2)}_{ZZZ}$ increases linearly with increasing chromophore concentration. In practice it is not the case because of the already mentioned chromophore aggregation. Therefore it is important to know how the bulk susceptibility depends on the NLO chromophore concentration to optimise its value. Systematic studies were done on the Disperse Red 1 (DR1) chromophore grafted on PMMA (polymethyl methacrylate) polymer. For this purpose side chain polymers with different DR1 substitution levels were synthesized.

DR1 chromophore (full name: *N*-Ethyl-*N*-(2-hydroxyethyl)-4-(4-nitrophenylazo) aniline) is one of the most studied quasi 1D charge transfer (CT) molecules with enhanced first hyperpolarizability. Typing just Disperse Red 1 (DR1) on Google website one obtains 1,450,000 references. Indeed, it can be considered as a model molecule for second order nonlinear optics, but not only. This molecule, due to the easiness to excite the double "–N=N–" bond shows an unusual ability to change its conformation from trans to cis form and vice versa. This transformation is connected with its volume change, just change of its rotational mobility. For example there is a ca. 10% decrease of the volume occupied by molecule passing from trans to cis form. As such conformational changes are connected with the change of π electron conjugation length, as result the material index of refraction is changing too. The trans-cis izomerization is believed also to be, at least in part, responsible for the mass transportation when e.g., the side chain polymers with grafted DR1 are subjected to inhomogeneous illumination of light [23–25]. Molecules from bright areas move to the dark ones. Trans-cis izomerization process is exploited also in all optical poling [26] of polymers and play also an important role in optical depoling [27,28].

The concentration dependence of another quadratic susceptibility tensor which describes the linear electro-optic effect was performed for another, similar chromophore which is Disperse Red 19 (DR19) dissolved in PMMA matrix (guest-host system) [29]. The authors observe almost a linear increase of the linear electro-optic coefficient r in function of DR19 weight concentration up to 30 w%, in agreement with Eq. (4). However, as it is discussed below, 30% w concentration corresponds to a relatively small chromophore mole concentration (<10%), because of its large molecular mass in comparison with that of the host monomer. In the present study we go far beyond this concentration and we measure the electronic part of quadratic susceptibility by using the SHG technique, which gives the fast electronic part of quadratic susceptibility. The experiments are done for side chain polymers, for which it is believed that the chromophore aggregation takes place at higher dye loading as in guest-host systems. Also both tensor components: the diagonal and the off diagonal are determined for each chromophore concentration studied.

Chemical Synthesis

Characterization Techniques

^{1}H NMR (500 MHz) spectra were recorded by the "Bruker Advance DRX-500" spectrometer using DMSO-d_6 as solvent. Chemical shifts are in ppm from the internal standard tetramethylsilane. *UV-VIS* measurements were performed at room temperature with a Perkin-Elmer UV/VIS/NIR Lambda 19 spectrometer. For solution using a pure silica liquid cell was used while thin films were deposited on the BK7 glass substrate. The *Differential Scanning Calorimetry*: Q20 DSC model was used to determine the glass transition temperatures (Tg) of all polymers. The sample was initially stabilized and after the first scan was made at the heating rate of 10°C/min up to 200°C then cooled to 20°C. Finally, a second scan was performed heating the sample at the rate of 10°C/min up to 200°C. The measured glass transition temperatures were in good agreement with the reported values [30,31]. *Size exclusion Chromatography:* The molecular weights and the molecular weight distribution of the polymers were taken with a system equipped with a guard column, followed by 2 columns, using the Spectra SYSTEM RI-150 and a Spectra SYSTEM UV2000 detectors. The solvent used was THF at a flow rate of 1 ml/min at 35°C. Polystyrene standards were used for calibration.

Materials Synthesis

4′-[(2-Methacryloyloxyethyl)ethylamino]-4-nitroazobenzene (M). 4′-[(2-Methacryloyloxyethyl)ethylamino]-4-nitroazobenzene was prepared by the procedure described below 4′-[(2-hydroxyethyl)ethylamino]-4-nitroazobenzene (2 g, 0.006 mol) and triethylamine (0.65 mL. 0.0065 mol) was dissolved in THF (35 mL). The solution was kept in an ice bath for 10 min. Then methacryloyl chloride (0.67 mL. 0.0065 mol) was added dropwise during 30 min to reaction mixture. The resulting mixture was stirred during 5 hours at 0°C. The solvent was removed by rotary evaporation, and the residue was washed with a solution of sodium carbonate (0.7 g) in water (40 mL). The solid was filtered, washed with water, and air dried. The solid was recrystallized from methanol. Crystals, yield 80%.

^{1}HNMR (DMSO-d_6), d(ppm): 8.16 (d, 2H, Ar), 7.87 (d, 2H, Ar), 7.85 (d, 2H, Ar), 6.81 (d, 2H, Ar), 6.1 (s, 1H, CH_2), 5.59 (s, 1H, CH_2), 4.39 (m, 2H, OCH_2), 3.72 (m, 2H, NCH_2), 3.57 (m, 2H, NCH_2), 1.93 (s, 3H, CH_3), 1.24 (m, 3H, CH_3).

Polymers Synthesis

Polymers with desired chromophore concentrations were obtained by free-radical polymerization in toluene. The polymerizations were carried out in 10 wt% toluene solution of 4′-[(2-methacryloyloxyethyl)ethylamino]-4-nitroazobenzene and

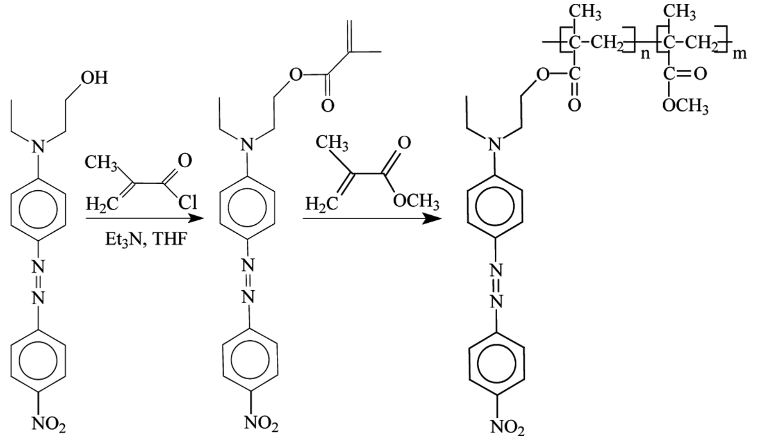

Figure 1. The synthesis route of studied PMMA-DR1 side chain polymers (n+m = 1).

methylmethacrylate with monomers initial mole ratios corresponding to the desired concentration. The polymerization processes were conducted using AIBN as a free radical initiator (1 wt% of monomers) and at 80°C for more than 24 h in argon atmosphere. The initial mixtures were degassed with repeated freeze cycles. The synthesized copolymers were isolated from the reaction solution by precipitation into methanol followed by reprecipitation from toluene into methanol and then dried at 70°C overnight. The copolymerization ratios were calculated on the basis of the integration ratio of ^{1}H NMR measurements; $\lambda_{max} = 276, 476$ in THF; in thin film on the glass slide $\lambda_{max} = 474$. The synthesis route of the studied PMMA-DR1 side chain polymers is shown in Figure 1. Polymers with mole fraction $C_m = n = 0.08, 0.15, 0.35, 0.50$, and 0.65 were obtained ($m = 1$-n).

Thin Film Deposition and Poling

Thin films of studied polymers were obtained by spin coating of filtered solutions on carefully cleaned BK7 glass slides. The principle of deposition (of the mixture with certain viscosity) is based on a homogeneous spreading out of the solution on the rotating substrate with an angular speed of 1000 rpm. The studied polymers are soluble in a large range of organic solvents. We used as solvent 1,1,2-trichlororethane for the quality of thin film formation. The same polymer concentrations of 100 g/l were used. Immediately after the deposition, the films were cured in an oven at 80°C and for 60 minutes in order to eliminate any remaining solvent. The thicknesses of thin films were of about 150 nm, as measured with a profilometer.

The required noncentrosymmetry in thin films was obtained by corona poling technique [4] (cf. also Kajzar *et al.* [3], Rau and Kajzar [32]). The poled films were placed at the distance of 20 mm from the discharge needle to which a high voltage of 6 kV was applied and during 3 mins. Then films were cooled down to room temperature under the applied poling field. This poling time is sufficient to obtain maximum of poling efficiency. All studied films were poled at the same conditions. No extra electrode on the substrate was used, as the conductivity of BK7 glass is sufficient to ensure the poling process. Figure 2 shows the optical absorption spectrum of a thin film of PMMA-DR1 $C_m = 0.5$ (50 mol%) before (solid line) and

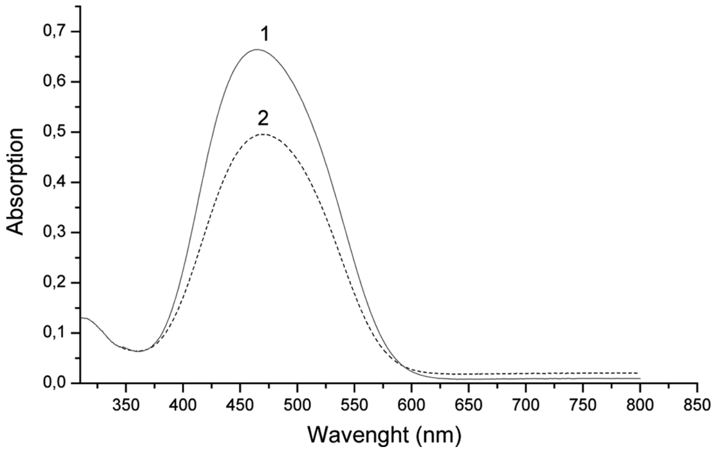

Figure 2. Optical absorption spectrum of a thin film of PMMA-DR1 50 mol% before (solid line) and after (dashed line) poling.

after (dashed line) poling. The ordering is observed by the decrease of the thin film optical absorption at normal incidence and the noncentrosymmetry by its red shift (cf. Page *et al.* [33]).

Second Harmonic Generation Experiments

The optical SHG measurements were done immediately after the poling in order to avoid decrease of NLO response by relaxation. The measurements were performed using a Q switched Nd:YAG laser, operating at 1.0642 mm fundamental wavelength with 13 ns pulse duration and 10 Hz repetition rate. The experimental set-up is shown schematically in Figure 3. The films were mounted on a goniometer, mounted on a rotation stage. The SHG intensities were collected in function of the incidence angle by rotating thin film around an axis perpendicular to the beam propagation direction and coinciding with. They were corrected for fundamental beam intensity variations by

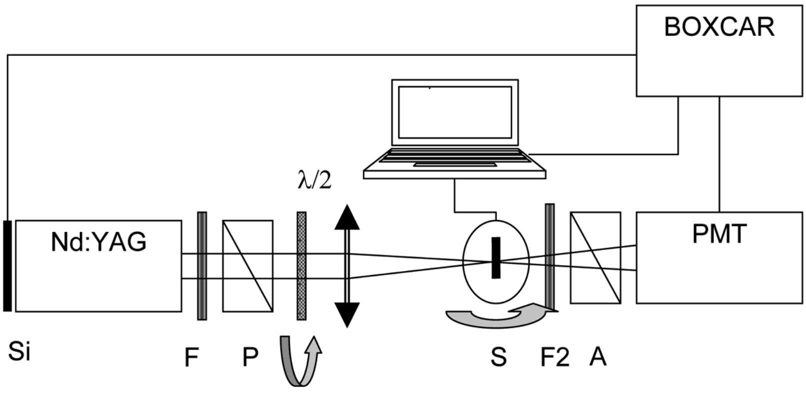

Figure 3. Schematic presentation of the experimental setup: F's – absorptive filters, P – polarizer, A – analyzer, S sample, Si – silicon photodiode, PMT – photomultiplier.

measuring it with a fast Si photodiode, located just behind the laser cavity. The intensity of fundamental beam was controlled by using calibrated neutral filters and the spurious light, coming particularly from flash lamps, was eliminated by using absorptive cut-off filters. Its polarization was controlled by the polarizer and half wavelength plate. By rotating the last the incident light polarization direction was moved smoothly without changing its intensity. Because the corona poling orient chromophores in the direction of the applied film, i.e., perpendicular to the thin film surface and existence of only two nonzero tensor components the range of incidence angle variation has to be very large, as at the normal incidence no SHG signal is observed.

The poled films exhibit ∞mm point symmetry. For this symmetry, if one takes account of the already mentioned Kleinman's relations [21], there are 2 nonzero $\chi^{(2)}$ tensor components: $\chi^{(2)}_{XXZ}$, $\chi^{(2)}_{ZZZ}$, where is the direction of the poling field (perpendicular to the thin film surface). Both can be measured by using two configurations of polarizations of input fundamental (f) and output harmonic (h) fields.

The output SHG intensity for a thin film is given by

$$I_{2\omega} = \frac{128\pi^3}{c^2}\left[\frac{\chi^{(2)}_{eff}(\theta)}{\Delta\varepsilon}\right]^2 |A(\theta)T(\theta)|^2 I^2_\omega \sin^2\frac{\Delta\varphi}{2} \qquad (6)$$

where $\chi^{(2)}_{eff}$ is an effective second order NLO susceptibility for a given propagation direction defined by the propagation angle θ, I_ω is the fundamental beam intensity and $A(\theta)$, $T(\theta)$ are, the factors arising from boundary and transmission conditions, respectively. $\Delta\varepsilon = \varepsilon_{2\omega} - \varepsilon_\omega$ is the dielectric constant dispersion between harmonic (2ω) and fundamental (ω) frequencies, c is the light velocity in vacuum and $\Delta\varphi$ is the phase mismatch between fundamental (f) and harmonic (h) beams:

$$\Delta\varphi = \varphi_\omega - \varphi_{2\omega} = \frac{4\pi\, l}{\lambda_\omega}(n_\omega\cos\theta_\omega - n_{2\omega}\cos\theta_{2\omega}) \qquad (7)$$

where $\Theta_{\omega\ (2\omega)}$ is the propagation angle at $\omega(2\omega)$ frequency, respectively and $n_{\omega(2\omega)}$ are the corresponding refractive indices.

In order to determine both nonzero tensor components two SHG measurements are to be performed in s-p and p-p fundamental – harmonic beam configurations. In the s-p polarization configurations the effective $\chi^{(2)}$ $(-2\omega\omega,\omega)$ susceptibility is given by:

$$\chi^{(2)}_{eff}(s-p) = \chi^{(2)}_{XXZ}\sin 2\theta^p_{2\omega} \qquad (8)$$

In the p-p fundamental – harmonic beam configuration it is given by

$$\chi^{(2)}_{eff}(p-p) = \chi^{(2)}_{ZZZ}\sin^2\theta^p_\omega \sin\theta^p_{2\omega} + \chi^{(2)}_{XXZ}\cos\theta^p_\omega(\cos\theta^p_\omega + 2\sin\theta^p_\omega\cos\theta^p_{2\omega}) \qquad (9)$$

Thus in the s-p polarization configuration one obtains unambiguously the $\chi^{(2)}_{XXZ}$ tensor component. This value, injected into Eq. (9) for SHG intensity formula (Eq. (6)) for p-p polarization configuration gives the value of the $\chi^{(2)}_{ZZZ}$ tensor component.

Equation (6), through Eqs. (7)–(9) shows that the SHG intensity depends on the propagation length, while it is important to measure it as the function of the

Table 1. Quadratic susceptibilities d_{sp} $(=\frac{1}{2}\chi^{(2)}_{XXZ}(-2\omega;\omega,\omega))$ and d_{pp} $(=\frac{1}{2}\chi^{(2)}_{ZZZ}(-2\omega;\omega,\omega))$ in pm/V as measured for different molar concentrations of the side chain polymer PMMA-DR1. Z is the poling direction. The numbers in brackets are standard deviations. For calibration the value of $d_{11} = 0.5$ pm/V [34] was used

Molar concentration (%)	d_{sp} (pm/V)	d_{pp} (pm/V)
8	29 (3)	72 (7)
15	35 (4)	111 (11)
35	12 (1)	52 (5)
50	19 (2)	57 (6)
65	18 (2)	59 (6)

incidence angle. We have done it by rotating the film around an axis perpendicular to the propagation direction and coinciding it. The incident angle SHG intensity dependence can be then fitted using Eq. (6), and respectively (8) or (9), depending on the fundamental – harmonic beam polarization.

As measuring absolute intensities is usually difficult one uses generally a standard with usually is a plate of an α-quartz single crystal. We used an y-cut single crystal and the SHG measurements we performed at the same experimental conditions. As value for $\chi^{(2)}_{XXX}$ we used that reported by Choy and Byer ($\chi^{(2)}_{XXZ} = 1$ pm/V at 1 064 nm [34]).

The measured values of $\chi^{(2)}_{XXZ}$ and $\chi^{(2)}_{ZZZ}$ tensor components for the studied thin films with different chromophore molar content expressed in percents, are listed in Table 1 for both tensor components, expressed in the commonly used notation: $d_{sp} = \chi^{(2)}_{XXZ}/2$ and $d_{pp} = \chi^{(2)}_{ZZZ}/2$. We observe an almost linear increase of these tensor components up to $C_m = 0.15$ (15 mol%) of DR1 and a decrease at higher concentration. For concentrations starting from $C_m = 0.35$ (35 mol%) the both tensor components stabilizes and remains constant.

A similar behavior is observed in the case of solution of lyotropic liquid crystals (LC) in water [35]. At low concentration only monomers are present. Their concentration increases linearly with LC concentration. At higher concentration micelles (a kind of aggregates) appear and their concentration is increasing rapidly, while the monomer concentration stabilizes and remains constant when increasing LC concentration. It means that all introduced LC molecules either attach to micelles or form new ones.

This result is very important from the point of view of practical applications of these materials in second order NLO devices. They show that there is an optimal concentration of chromophores. Its increase leads to aggregation, decrease of NLO response and as a harmful consequence, the light scattering.

6. Conclusion

The present study confirms earlier funding of Robinson and Dalton [29] that there is an optimal chromophore concentration C_{opt} in electro-optic polymers for which the bulk quadratic susceptibility reaches its maximum. For concentrations smaller than C_{opt} both susceptibilities follow linearly the chromophore concentration, as it should be. For higher concentrations ($C > C_{opt}$) $\chi^{(2)}$ susceptibility decreases. The maximum is reached at relatively low molar concentration of about $C_m = 0.15$ or very close to this value, as for the next concentration of 35 mol% it falls to less than one half of the maximum value. Both $\chi^{(2)}$ components: the diagonal and the off diagonal follow similar dependence on concentration and the ratio $\chi^{(2)}_{pp}/\chi^{(2)}_{sp}$ remains constant within experimental accuracy with a value of about 3. It corresponds to a moderate poling, characteristic for isotropic polymers, as it is the case here (free gas model).

The difference with the earlier study of Robinson and Dalton concerning the concentration dependence of quadratic susceptibility can be easily explained. Both molecules exhibit very similar molecular structure (cf. Fig. 4) and we can expect very similar behaviour. In fact it arises from the fact how the chromophore concentration is labelled. Although $C_w = 0.3$ (30 wt%) seems to be a high concentration, in fact it is small if we look at the number of chromophores introduced to the system (mole fraction). Thus to compare our findings with their we have to use the same concentration description. Indeed, using weight concentration dependence may be misleading because it doesn't refer directly to the number of substituted monomer-chromophore segments and the number of non substituted monomers in polymer chain. A simple relation between the molar and the weight concentration can be easily derived for a side chain polymer, which is given by

$$C_m = C_w \frac{R}{1 + (1 - R)C_w} \tag{10}$$

where

$$R = \frac{M_{mon}}{M_{seg}} \tag{11}$$

is the ratio of molecular mass of the unsubstituted monomer (M_{mon}) to the segment monomer + chromophore (M_{seg}).

In our case (PMMA-DR1 side chain polymer) $M_{seg} = 382.42$, $M_{mon} = 100.12$, and $R = 0.26$. Thus for the maximum concentration of DR19 in PMMA studied by Robinson and Dalton $C_w = 0.3$ we obtain a molar concentration of $C_m = 0.064$, what corresponds to a small substitution rate, thus to a small aggregation level. For DR19, whose molar mass is a little larger, this value will be a little smaller. In fact Lei *et al.* [36] (see also Kuzyk *et al.* [37]) consider occurrence of aggregation

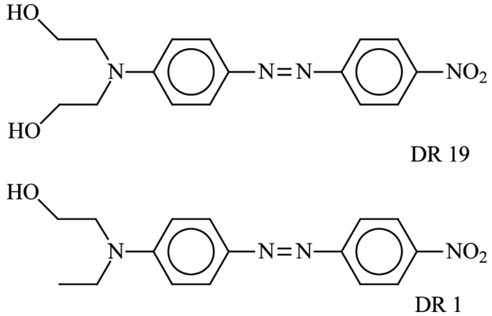

Figure 4. Chemical structures of DR1 and of DR19.

at $C_w = 0.15$ of DR1 in PMMA (guest-host). M. Kuzyk [38] sets the limit at $C_w = 0.12$ for this system. It is commonly believed that in side chain polymers, because of limited mobility, aggregation takes place at higher chromophore concentration. Thus the observed here $C_m = 0.15$ (15 mol %) limit looks as a very reasonable and realistic one.

Acknowledgments

One of the authors (FK) would like to thank Prof. M. G. Kuzyk from Washington State University ate Pullman, USA, for a fruitful discussion.

References

[1] (1997). *Poled Polymers and Their Application to SHG and EO Devices*, Myata, S. & Sasabe, H. (Eds.), Gordon & Breach Sc. Publ: Amsterdam.

[2] Kajzar, F., Jen, A., & Lee, K. S. (2003). *Polymeric Materials and Their Orientation Techniques for Second-Order Nonlinear Optics*, in Polymers for Photonics Applications I, Lee, K. S. & Wegner, G. Eds: Advances in Polymer Sc: Springer Verlag, Heidelberg, 161, 1.

[3] Dalton, L. R. (2001). *Advances in Polymer Science*, in Polymers for Photonics Applications I, in Lee, K. S. & Wegner, G. Eds: Advances in Polymer Sc: Springer Verlag, Heidelberg, 161 1(2003), Springer-Verlag, Heidelberg, 158, 1.

[4] Comizzoli, B. (1987). *J. Electrochem. Soc.: Solid Science and Technology*, *134*, 424.

[5] Charra, F., Kajzar, F., Nunzi, J. M., Raimond, P., & Idiart, E. (1993). *Opt. Lett.*, *18*, 941.

[6] Aktsipetrov, O. A., Akhmediev, N. N., Mishina, N. N., & Novak, V. R. (1983). Soviet Phys. *JETP Lett.*, *37*, 207.

[7] Bosshard, C. & Kupfer, M. (1996). *Oriented Molecular Systems, in* Organic Thin Films for Waveguiding Nonlinear Optics: Advances in Nonlinear Optics Kajzar, F. & Swalen, J. Eds., Gordon & Breach Sc. Publ., p. 163.

[8] Kajzar, F. & Swalen, J. (1996). (Eds), *Organic Thin Films for Waveguiding Nonlinear Optics: Advances in Nonlinear Optics*, Gordon & Breach Sc. Publ.: Amsterdam.

[9] Gonin, D., Noël, C., & Kajzar, F. (1996). *Liquid Crystalline Polymers*, in Kajzar, F. & Swalen, J. Eds., Organic Thin Films for Waveguiding Nonlinear Optics: Advances in Nonlinear Optics, Gordon & Breach Sc. Publ.: Amsterdam, p. 221.

[10] Kajzar, F. & Noel, C. (1998). *Adv. Mat. Opt. Electron.*, *8*, 247.

[11] Le Moigne, J. (1996). *Epitaxy and Single Crystal Growth*, in Organic Thin Films for Waveguiding Nonlinear Optics: Advances in Nonlinear Optics, Kajzar, F. & Swalen, J. Eds., Gordon & Breach Sc. Publ.: Amsterdam, p. 289.

[12] Favaretto, L., Barbarella, G., Rãu, I., Kajzar, F., Caria, S., Murgia, M., & Zamboni, R. (2009). *Opt. Express*, *17*, 2557–2564.

[13] Facchetti, A., Annoni, E., Beverina, L., Beverina, L., Morone, M., Zhu, P., Marks, T. J., & Pagani, G. A. (2004). *Nature Materials*, *3*, 910.

[14] Kajzar, F., Okada-Shudo, Y., Meritt, C., & Kafafi, Z. (2001). *Synth. Metals*, *117*, 189.

[15] Chen, D., Fetterman, H. R., Chen, A., Steier, W. H., Dalton, L. R., Wang, W., & Shi, Y. (1997). *Appl. Phys. Lett.*, *70*, 3335.

[16] Shi, Y., Zhang, Ch., Zhang, H., Bechtel, J. H., Dalton, L. R., Robinson, B. H., & Steier, W. H. (2000). *Science*, *288*(5463), 119–122.

[17] Blau, G., Ruiz, L., Casablanca, P., Vitrant, G., Chollet, P. A., & Kajzar, F. (1996). *Electro-optic Modulation in Organic Waveguides Using GratingCouplers*, in Photoactive Organic Materials: Science and Application, Kajzar, F., Agranovich, V. M., & Lee, C. Y.-C. Kluwer Academic Publishers: Dordrecht, pp. 275–280.

[18] Alshikh Khalil, M., Vitrant, G., Raimond, P., Chollet, P. A., & Kajzar, F. (1999). *Opt. Commun.*, *170*, 281–284.

[19] Khalil, M. A., Vitrant, G., Raimond, P., Chollet, P., & Kajzar, F. (2000). *Appl. Phys Lett.*, *77*, 3713–3715.

[20] Rodríguez, A., Vitrant, G., Chollet, P. A., & Kajzar, F. (2001). *Appl. Phys. Lett.*, *79*, 461–463.

[21] Kleinman, D. A. (1962). *Phys. Rev.*, *126*, 1977–1979.

[22] Rau, I. & Kajzar, F. (2008). *Nonl. Opt. Quant. Opt.*, *38*, 99–140.

[23] Natansohn, A. & Rochon, P. (1999). *Adv. Mater.*, *11*, 1387–1391.

[24] Kim, D. Y., Tripathy, S. K., Li, L., & Kumar, J. (1995). *Appl. Phys. Lett.*, *66*, 1166–1168.

[25] Lefin, P., Fiorini, C., & Nunzi, J.-M. (1998). *Pure Appl. Opt.*, *7*, 71–82.

[26] Charra, F., Kajzar, F., Nunzi, J. M., Raimond, P., & Idiart, E. (1993). *Optics Lett.*, *18*, 941–944.

[27] Large, M., Kajzar, F., & Raimond, P. (1998). *Applied Phys. Lett.*, *73*, 3635–3637.

[28] Combellas, C., Kajzar, F., Mathey, G., Petit, M. A., & Thiebault, A. (2000). *Chem. Phys.*, *252*, 165–177.

[29] Robinson, B. H. & Dalton, L. R. (2000). *Journal of Physical Chemistry A*, *104*(20), 4785–4795.

[30] Narita, M., Hoshino, F., Mouri, M., Tsuchimori, M. T., & Watanabe, O. (2007). *Macromolecules*, *40*, 623–629.

[31] Ho, M. S., Natansohn, A., & Rochon, P. (1995). *Macromolecules*, *28*(18), 6124–6127.

[32] Rau, I. & Kajzar, F. (2008). *Nonl. Opt. Quant. Opt.*, *38*, 99–140.

[33] Page, R. H., Jurich, M. C., Reck, B., Sen, A., Twieg, R. J., Swalen, J. D., Bjorklund, G. C., & Wilson, C. G. (1990). *J. Opt. Soc. Am. B*, *7*, 1239.

[34] Choy, M. & Byer, R. L. (1976). *Phys. Rev. B.*, *14*, 1693.

[35] Oswald, P. & Pieranski, P. (2000). *Les Cristaix Liquides: Concepts et Propriétés Physiques Illustrés par des Expériences*, Gordon and Breach Science Publishers: Paris, Vol. 1., 51.

[36] Lei, D., Runt, J., Sarari, A., & Newnham, R. E. (1987). *Macromolecules*, *20*, 1797.

[37] Kuzyk, M. G., Sohn, J. E., & Dirk, C. W. (1990). *J. Opt. Soc. Am. B*, *7*(5), 843–858.

[38] Kuzyk, M. G. private communication.